Ionic Mechanism of Postsynaptic Inhibition

J. C. Eccles

The body and dendrites of a nerve cell are specialized for the reception and integration of information which is conveyed as impulses that are fired from other nerve cells along their axons. In a diagrammatic drawing of a nerve cell (Fig. 1*A*) it is seen that impinging on the surface of the cell are numerous small knob-like endings of fine fibers which are, in fact, the terminal branches of axons from other nerve cells. Communication between nerve cells occurs at these numerous areas of close contact, or *synapses*, the name first applied to them by Sherrington, who laid the foundations of what is often called synaptology. We owe to Dale and Loewi the concept that transmission across synapses is effected by the secretion of minute amounts of specific chemical substances that act across the synapse. The cable-like transmission of impulses over the surfaces of nerve cells and their axons ceases abruptly at the synaptic contact between cells, but may begin again on the other side of the synapse.

The high resolving power of electron microscopy gives essential information on those structural features of synapses that are specially concerned with this chemical phase of transmission. For example, in Fig. 1, *B* and *C*, we can see the membrane, about 70 angstroms thick, that encloses the expanded axonal terminal or synaptic knob. These knobs contain numerous small vesicular structures, the synaptic vesicles, that are believed to be packages of the specific chemical substances concerned in synaptic transmission. Some of these vesicles are concentrated in zones on the membrane that fronts the synaptic cleft, which is the remarkably uniform space, about 200 angstroms across, that is indicated by arrows in Fig. 1*B*. The chemical transmitter substance is released from the synaptic knob into the cleft and acts on the subsynaptic membrane. Since synaptic transmission has to occur across the synaptic cleft that is interposed between the presynaptic and postsynaptic components of the synapse, it might appear that the synaptic cleft is merely a barrier to transmission, but we shall see later that it must not be too narrow, else it will unduly impede the flow of the postsynaptic electric currents that provide the essential expression of synaptic actions of all kinds; in its dimensional design the synaptic cleft approaches optimum efficiency.

The experimental investigation of synaptic transmission was transformed in 1951 (*1*, *2*) by the introduction of the technique of recording electrically from the interior of nerve cells. It is possible to insert into nerve cells a fine glass pipette having a tip diameter of about 0.5 micron and filled with a conducting salt solution such as concentrated potassium chloride. If this is done with rigid precautions of mechanical fixation, the cell membrane is believed to seal around the glass microelectrode, preventing the flow of a short-circuiting current from the outside to the inside of the cell. Many impaled nerve cells appear to behave normally even for hours. In the central nervous system one is of course searching blindly for cells, but, by utilizing clues provided by the electric field potentials radiating from activated cells, a great many cells can be located and successfully impaled in a single experiment. In Fig. 2 a microelectrode has been drawn on a microphotograph of one of the large nerve cells or motoneurons that innervates muscle, but for illustrative purposes it is magnified about five times, relative to the motoneuron. It was a fortunate choice that our first investigations were on motoneurons, because intracellular investigations have proved to be much easier and more rewarding in these cells than in any other kind of mammalian nerve cell.

Ionic Composition and Electrical Charges

I must now digress briefly in order to give an account of the ionic composition of nerve cells and of the electrical charges on their surfaces, because both these features are essentially concerned in synaptic action. As shown in Fig. 3*A*, the surface membrane of a nerve cell separates two aqueous solutions that have very different ionic composition. The external concentrations would be virtually the same as for a protein-free filtrate of blood plasma. The internal concentrations are approximate, being derived more indirectly, from investigations on the equilibrium potentials for some physiological processes that are specifically produced by one or two ion species, and also from more general considerations. Within the cell, sodium and chloride ions are at a lower concentration than outside, whereas with potassium there is an even greater disparity—almost 30-fold—in the reverse direction. The equilibrium potentials for each species of ion are the membrane potentials at which there is equality of diffusion inward and outward. Under resting conditions potassium and chloride ions move through the membrane much more readily than sodium. The formal electrical diagram of Fig. 3*B* gives, under resting conditions, the electrical properties of the surface membrane of a motoneuron as "seen" by a microelectrode inserted intracellularly, as in Fig. 2. A battery of about −70 millivolts (inside negativity) with an in-series resistor is in parallel with a capacitance (*3–5*). Figure 3*C* shows diagrammatically the way in which a metabolically driven pump can compensate for the unbalance in diffusion of

The author is professor of physiology at Australian National University, Canberra. This article is adapted from the lecture he delivered in Stockholm, Sweden, 10 December 1963, when he received the Nobel prize in medicine and physiology, a prize which he shared with Alan Lloyd Hodgkin and Andrew Fielding Huxley. It is published with the permission of the Nobel Foundation. It will also be included in the complete volume of Nobel lectures in English which is published yearly by the Elsevier Publishing Company, Amsterdam and New York.

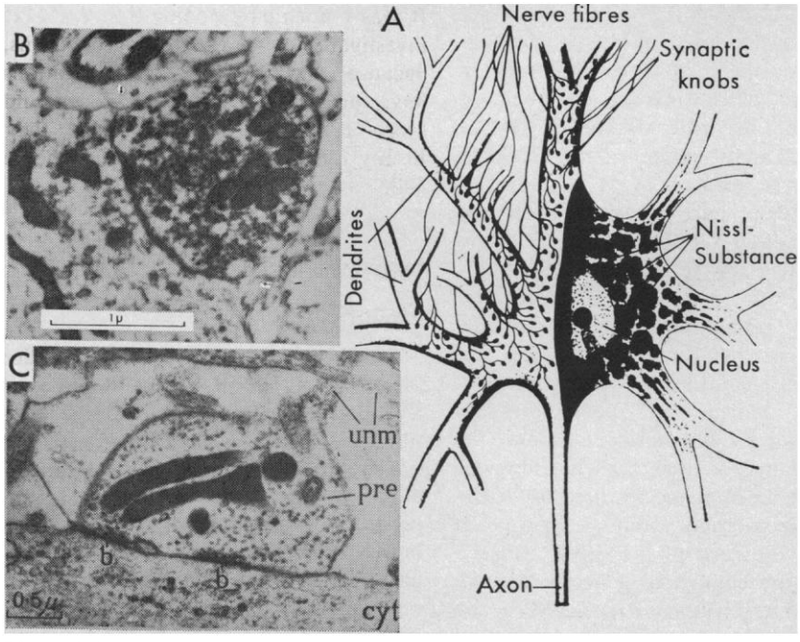

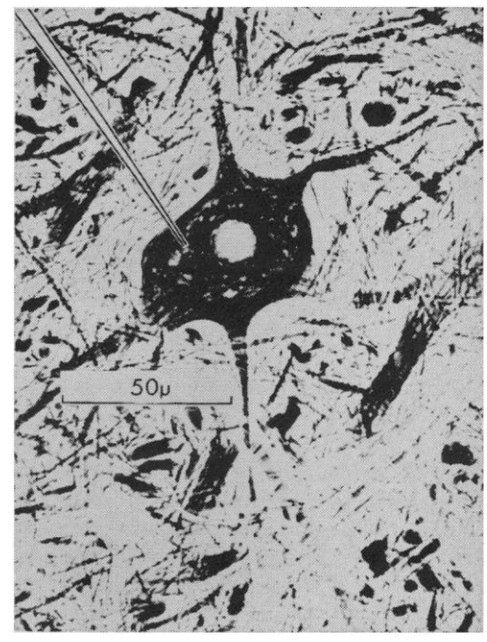

Fig. 1 (left). *A*, Diagrammatic drawing of a neuron, showing dendrites and axon radiating from the cell body or soma that contains the nucleus. Several fine nerve fibers are shown branching profusely and ending in synaptic knobs on the body and dendrites (Jung, *29*). *B*, Electron micrograph of a synaptic knob separated from the subsynaptic membrane of a nerve cell by a synaptic cleft (marked by arrows) about 200 angstroms wide. In some areas the vesicles are seen to be concentrated close to the synaptic surface of the knob, and there is an associated increase in membrane density on either side of the cleft (Palay, *30*). *C*, Electron micrograph of an inhibitory synapse that is formed by a synaptic knob (*pre*) of a basket cell on the soma (*cyt*) of a hippocampal pyramidal cell (Hamlyn, *31*). Fig. 2 (right). Photomicrograph of a motoneuron with radiating dendrites and axon, as in Fig. 1*A*, but superimposed on it is a drawing of a microelectrode shown as it would be located for intracellular recording, though on a scale about 5 times that of the motoneuron (Brock, Coombs, and Eccles, *2*).

sodium and potassium ions across the surface membrane. With nerve cells the situation is believed to be very similar to that so rigorously investigated with giant axons, peripheral nerve fibers, and muscle fibers by Hodgkin, Huxley, and their colleagues (*6*).

Synaptic Action

The simplest example of synaptic action is illustrated in Fig. 4, where a single synchronous synaptic bombardment diminishes the electric charge on the cell membrane. A rapid rise to the summit is followed by a slower, approximately exponential, decay. This depolarization becomes progressively larger in *A* to *C* as the number of activated synapses increases, there being in fact a simple summation of the depolarizations produced by each individual synapse. In the much faster records *D* to *G* it is seen that, when above a critical size, the synaptic depolarization evokes, at the double arrows, the discharge of an impulse, just as occurs in peripheral nerve. The only effect of strengthening the synaptic stimulus in *E* to *G* was the earlier generation of the impulse, which in every case arose when the depolarization reached 18 millivolts. The synapses that in this way excite nerve cells to discharge impulses are called excitatory synapses, and the depolarizing potentials that excitatory synapses produce in the postsynaptic membrane are called excitatory postsynaptic potentials (or EPSP). There has now been extensive investigation of a wide variety of nerve cells in the central nervous system, and in every case synaptic transmission of impulses is due to this same process of production of EPSP's, which in turn generate impulse discharge on attaining a critical level of depolarization (*5, 7–9*).

In Fig. 4*H* changing the membrane potential by means of a background current altered the size of the EPSP and even caused its reversal when the membrane potential was reversed. These findings of an approximately linear relationship of membrane potential to size of EPSP are in good accord with the hypothesis that the subsynaptic membrane under the excited synapses acts as a virtual short-circuit of the postsynaptic membrane potential, and that the excitatory postsynaptic potential is generated by ions moving down their electrochemical gradients, and not by such a process as the activation of an ionic pump (*5, 10, 11*).

In this lecture I am primarily concerned with a second class of synapses that oppose excitation and tend to prevent the generation of impulses by excitatory synapses; hence they are called inhibitory synapses. There is general agreement that these two basic modes of synaptic action govern the generation of impulses by nerve cells. As shown in Fig. 5, *A–D*, activation of inhibitory synapses causes an increase in the postsynaptic membrane potential. This inhibitory postsynaptic potential (IPSP) is virtually a mirror image of the EPSP (Fig. 5*E*) (*12*). The effects of individual inhibitory synapses (Fig. 5, *A–C*) on a nerve cell summate in exactly the same way that the effects of excitatory synapses do; and of course the inhibition of excitatory synaptic action is accounted for by the opposed action on the potential of the postsynaptic membrane (*2, 5, 8, 13, 14*).

The effects produced in the size and direction of the IPSP by varying the initial membrane potential (Fig. 5*G*) correspond precisely to the changes that would be expected if the currents generating the IPSP were due to ions moving down their electrochemical

gradients, there being a reversal of the current at about −80 millivolts (*5, 10, 15, 16*). These currents would be caused to flow by increases in the ionic permeability of the subsynaptic membrane that are produced under the influence of the inhibitory transmitter substance. The conditions causing the generation of an IPSP are shown in the formal electrical diagram of Fig. 5*F* where activation of the synapses closes the switch shown in the right-hand element of the diagram. Figure 6*B* shows diagrammatically the flow of current under an activated inhibitory synapse—outward through the subsynaptic membrane along the synaptic cleft and so circling back to hyperpolarize the postsynaptic membrane by inward flow over its whole surface; this flow is the reverse of that for an excitatory synapse (Fig. 6*A*). The outwardly directed current across the inhibitory subsynaptic membrane could be due to the outward movement of a cation, such as potassium, or the inward movement of an anion, like chloride, or to such a combination of anionic and cationic movements that there is a net outward flow of current driven by a battery of about −80 millivolts in series with a fairly low resistance.

Figure 6*C* serves to illustrate the simplest findings on the EPSP and the IPSP and their interaction. The approximate equilibrium potentials for sodium, chloride, and potassium ions are shown by the horizontal lines, the equilibrium potential for chloride ions being assumed to be identical with the resting membrane potential. In the left part of diagram *C* the EPSP is seen to be large enough to generate a spike potential, the course of the EPSP in the absence of the spike being shown by the broken line. In the right part of diagram *C* there is an initial IPSP (solid line), which is seen to diminish the depolarization produced by the same synaptic excitation, so that it no longer is adequate to generate a spike (*13*).

Investigations on Ionic Mechanisms

Experimental investigations on the ionic mechanisms involve altering the concentration gradient across the postsynaptic membrane for one or other species of ion normally present, and, in addition, employing a wide variety of other ions in order to test the ionic permeability of the subsynaptic membrane. With the inhibitory synapses on invertebrate nerve and muscle cells, the investigations are usually performed on isolated preparations. Changes in relative ionic concentration across the post-

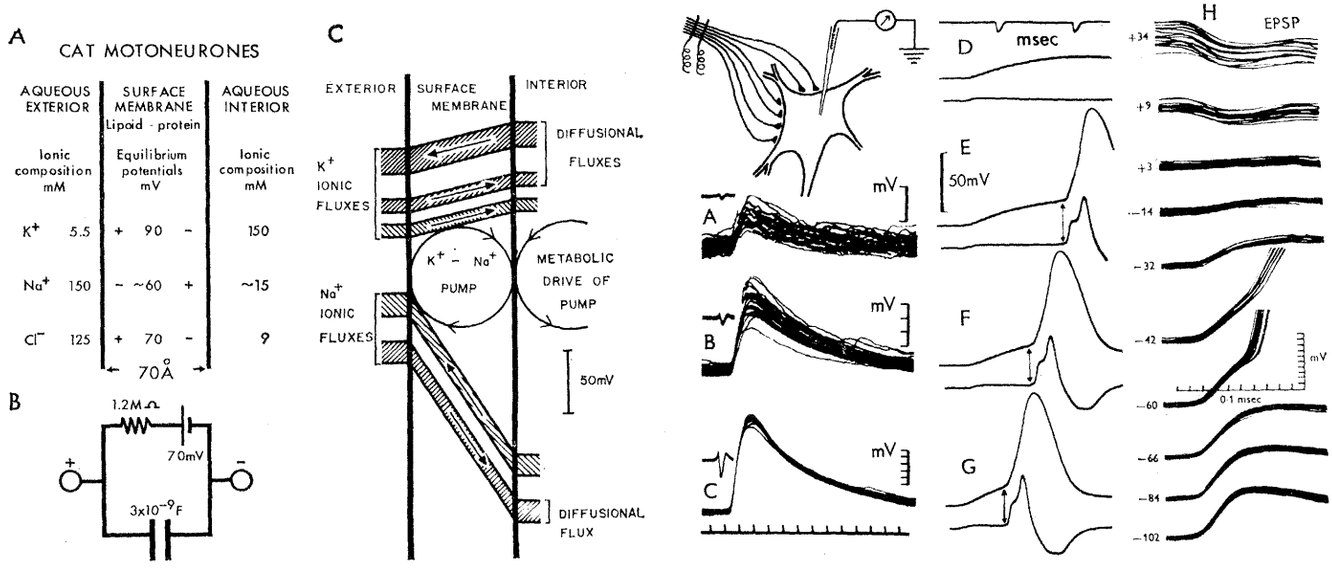

Fig. 3 (left). *A*, The approximate values are shown for the extracellular and intracellular ionic composition of cat motoneurons. Also shown are the approximate equilibrium potentials for K^+, Na^+, and Cl^- ions across the lipoid-protein cell membrane, which is about 70 angstroms thick. *B*, Formal electrical diagram of the approximate electrical characteristics of the surface membrane of a motoneuron as tested by applying electric pulses through a microelectrode in the soma. *C*, Diagrammatic representation of K^+ and Na^+ fluxes through the surface membrane in the resting state. The slopes in the flux channels across the membrane represent the respective electrochemical gradients. At the resting membrane potential (—70 mv) the electrochemical gradients, as drawn for the K^+ and Na^+ ions, correspond, respectively, to the potentials which are 20 millivolts more positive and about 130 millivolts more negative than the equilibrium potentials (note the potential scale). The fluxes due to diffusion and those due to operation of the pump are distinguished by the direction of hatching. The outward diffusional flux of Na^+ ions would be less than 1 percent of the inward flux and thus too insignificant to be indicated as a separate channel in the diagram, where the magnitudes of the fluxes are indicated by the widths of the respective channels (Eccles, *5*). Fig. 4 (right). *A–C*, Excitatory postsynaptic potentials obtained in a biceps-semitendinosus motoneuron with afferent volleys of different size, the experimental arrangements being shown schematically in the inset diagram. The inset records (negativity downward) at left of the main records show the afferent volley recorded near the entry of the dorsal nerve roots into the spinal cord. Records of EPSP's are taken at an amplification that decreases in steps from *A* to *C* as the response increases. All records are formed by superposition of about 40 faint traces (Coombs, Eccles, and Fatt, *15*). *D–G*, Intracellularly recorded potentials of a gastrocnemius motoneuron (resting membrane potential, —70 mv) evoked by monosynaptic activation that was progressively increased from *D* to *G*. The lower traces are the electrically differentiated records, the double-headed arrows indicating the onsets of the IS spikes in *E* to *G* (Coombs, Curtis, and Eccles, *3*). *H*, Intracellular ESPS's produced by a maximum afferent volley, as in *C*, but at the indicated membrane potentials, which were changed from the resting level of —66 millivolts by the application of steady background currents through one barrel of a double microelectrode, the other being used for recording. Spike potentials were evoked at membrane potentials of —42 and —60 millivolts (Coombs, Eccles, and Fatt, *11*).

synaptic membrane are readily effected by altering the ionic composition of the external medium. This method is not suitable for studying mammalian motoneurons, or, indeed, any neurons of the mammalian central nervous system. Instead, the procedure of electrophoretic injection of ions out of the impaling microelectrode has been employed to alter the ionic composition of the postsynaptic cell. For example, the species of anions that can pass through the inhibitory membrane have been recognized by injecting one or other species into a nerve cell and seeing if the increase in intracellular concentration effects a change in the inhibitory postsynaptic potential. These injections are accomplished by filling microelectrodes with salts containing the anions under investigation. When the microelectrode is inserted into a nerve cell, a given amount of the anion can be injected electrophoretically into the cell by passing an appropriare current through the microelectrode (*15*, *17*).

In Fig. 7 the IPSP in record *A* was changed to a depolarizing potential (record *B*) by the addition of about 5 pica equivalents of chloride ions to the cell, which would more than triple the concentration, whereas after the injection of more than twice this amount of sulfate ions into another cell, the IPSP was unchanged (Fig. 7, *E* and *F*). This simple test establishes that, under the action of the inhibitory transmitter, the subsynaptic membrane momentarily becomes permeable to chloride ions, but not to sulfate. In Fig. 7, *I* and *J*, it may be seen that, with two types of inhibitory synaptic action, the inhibitory membrane was permeable to nitrite ions, and recovery from the effect of the ionic injection was complete in about 2 minutes (*18*).

Ionic Mechanism of Inhibition

It is essential to recognize that Fig. 7 exemplifies two quite distinct processes of ionic exchange. Firstly, the ionic permeability of the whole postsynaptic membrane controls the intracellular ionic composition and is responsible for the recovery after ionic injections that occupies 2 minutes in Fig. 7, *I* and *J*. Secondly, the specialized subsynaptic areas under the influence of the inhibitory transmitter develop for a few milliseconds a specific ionic permeability of a much higher order. This second process is responsible for the ionic fluxes that give the inhibitory subsynaptic currents that are our present concern.

Some 33 anions have been tested on motoneurons by my colleagues in Canberra (*15*, *18*, *19*), and, as shown by the horizontal bars in Fig. 8, the permeable anions (solid bars) are distinguished by having small diameters in the hydrated state, whereas the impermeable anions are larger. The formate ion is exceptional in that it lies outside the main sequence; otherwise the inhibitory membrane is permeable to all anions that, in the hydrated state, have a diameter not more than 1.14 times that of the potassium ion—that is, not more than 2.85 angstroms, the diameter of the chlorate ion. The ion diameters in Fig. 8 are derived from limiting ion conductances in accordance with Stokes's law, on the assumption that the hydrated ions are spherical. Possibly the hydrated formate ion may have an ellipsoid shape and hence be able to negotiate membrane pores that

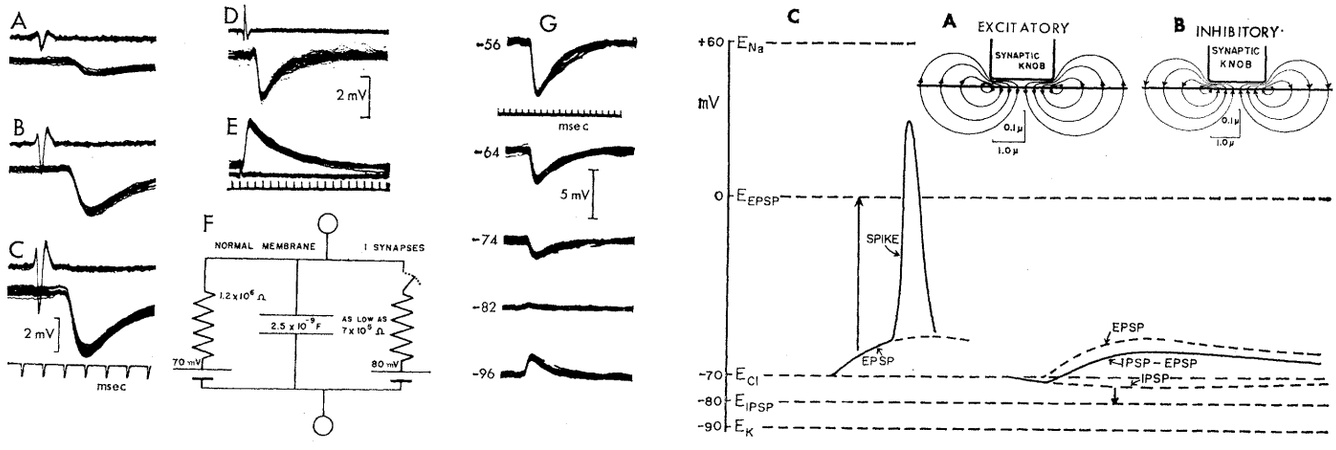

Fig. 5 (left). *A–C*, Lower records give intracellular responses of inhibitory postsynaptic potentials of a motoneuron produced by an afferent volley of progressively increasing size, as shown in the upper traces, which are dorsal root records, downward deflections signaling negativity. All records are formed by the superposition of about 40 faint traces (Eccles, *14*). *D*, Inhibitory postsynaptic potentials similarly recorded at lower sweep speed from another motoneuron, *E* being its monosynaptic EPSP's (Curtis and Eccles, *12*). *F*, Formal electrical diagram of the membrane of a motoneuron. At left is the normal membrane, as in Fig. 2*B*; at right are the inhibitory subsynaptic areas of the membrane that, when activated, give the IPSP. Maximum activation of these areas would be symbolized by a momentary closure of the switch. *G*, Inhibitory postsynaptic potentials recorded intracellularly from a motoneuron with a double-barreled microelectrode, the membrane potential being changed to the indicated values by a steady background current through one barrel, as in Fig. 4*H* (Coombs, Eccles, and Fatt, *15*). Fig. 6 (right). *A*, Diagram showing an activated excitatory synaptic knob. As indicated below the diagram, the synaptic cleft is shown at a scale for width 10 times that for length. The current passes inward along the cleft and in across the activated subsynaptic membrane. Elsewhere, as shown, it passes outward across the membrane, generating depolarization of the EPSP. *B*, Diagram showing the reverse direction of current flow for an activated inhibitory synaptic knob. *C*, Diagram showing the equilibrium potentials for sodium (E_{Na}), potassium (E_K), and chloride (E_{Cl}) ions, as given in Fig. 3*A* together with the equilibrium potential for postsynaptic inhibition (E_{IPSP}). The equilibrium potential for the EPSP (E_{EPSP}) is shown at zero. To the left, an EPSP generates a spike potential at a depolarization of about 18 millivolts (see Fig. 4, *E–G*). To the right, an IPSP and an EPSP are shown, alone (dashed lines) and then interacting (solid line). As a consequence of the depressant influence of the IPSP, the EPSP that alone generated a spike (at left) no longer is able to attain the threshold level of depolarization—that is, the inhibition has been effective.

block smaller spherical ions. In Japan and England similar series of permeable and impermeable ions, even the anomalous formate permeability, have been observed in comparable investigations on inhibitory synapses in fish (*20*), toads (*21*), and snails. It will certainly be remarkable if the ionic mechanism of central inhibition is exactly the same throughout the whole animal kingdom.

Effects of Cation Injections

In the original investigation (*5*, *15*) of the postulate that the net flux of potassium ions contributes substantially to the inhibitory current, we compared the effects of passing depolarizing currents out of intracellular microelectrodes that were filled either with sodium sulfate or potassium sulfate. It was assumed that the current is carried out of the microelectrode largely by the highly concentrated cations therein (sodium or potassium as the case may be), and that it is passed across the cell membrane partly by an outward flux of cations (largely potassium) and partly by an inward flux of anions (largely chloride). The injection of sodium ions was very effective in inverting the IPSP to a depolarizing response (Fig. 9, *A* and *B*), there being a very large displacement of the inhibitory equilibrium potential in the direction of depolarization (Fig. 9, *D* and *E*), and recovery (Fig. 9, *C–E*) was about five times slower than with the similar displacement produced by injection of such permeable anions as chloride or nitrite (Fig. 7, *I* and *J*). On the other hand, after the injection of potassium ions the displacement of the equilibrium potential was much less and recovery was as rapid as after anion injections.

Originally we attributed this large and prolonged displacement of the IPSP by the sodium injection to the depletion of intracellular potassium, which would cause just such an effect if the flux of potassium ions were importantly concerned in the generation of the IPSP. However, this interpretation must now be rejected because, on the basis of the hypothesis of uniform electric field across the membrane (the Goldman equation), quite different curves would be expected when the size of the IPSP is plotted against membrane potential (*9*, *22*). The family of curves plotted in Fig. 9*D* after a sodium ion injection is precisely what would be expected if the internal concentration of chloride ions were the determining factor. Hence, after the sodium injection it appears that the raised intracellular chloride concentration recovers at a rate which is much slower than the usual rate of diffusional recovery (for example, after chloride injections), being in fact as slow as the recovery from the changes that the sodium injection produces in the spike potential and the after-hyperpolarization.

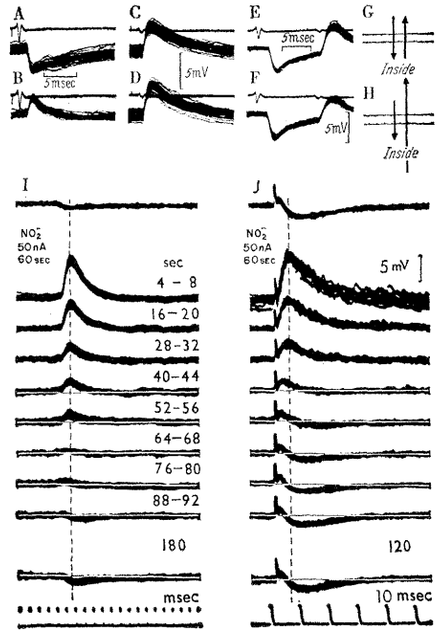

Fig. 7. *A* and *B* are IPSP's and *C* and *D* are EPSP's generated in a biceps-semitendinosus motoneuron by afferent volleys, as in Fig. 4, *G* and *H*, respectively. *A* and *C* were first recorded, then a hyperpolarizing current of 2×10^{-8} ampere was passed through the microelectrode, which had been filled with 3*M* KCl. Note that the injection of chloride ions converted the IPSP from a hyperpolarizing (*A*) to a depolarizing (*B*) response, while the EPSP was not appreciably changed (*C* and *D*). Passing a much stronger hyperpolarizing current (4×10^{-8} amp for 90 seconds) through a microelectrode filled with 0.6*M* K_2SO_4 caused no significant change (*E*, *F*) in either the IPSP or the later EPSP. *G* and *H* represent the assumed fluxes of chloride ions across the membrane before (*G*) and after (*H*) the injection of chloride ions, which, as shown, greatly increases the efflux of chloride (Eccles, *24*). *I–J*, Effects of electrophoretic injection of NO_2^- ions into motoneurons. *I*, Ia IPSP in a PBST motoneuron evoked by a quadriceps Ia volley. *J*, Renshaw IPSP in a motoneuron, the innervation of which was not identified, induced by a maximal L_7 ventral root stimulation. Records in row 1 (*I*, *J*, top row) show control IPSP's evoked before the injection. Records in rows 2 to 9 show IPSP's at the indicated times (identical in *I* and *J*), after the injection of NO_2^- ions, induced by the passage of a current of 5×10^{-8} ampere for 60 seconds. The records in row 10 are IPSP's at the end of recovery. Note the difference in time scales for *I* and *J*. All records were formed by the superposition of about 20 faint traces (Araki, Ito, and Oscarsson, *18*).

When the ionic composition of a motoneuron is modified, as in Fig. 9, the most significant information about the IPSP is the displacement of its equilibrium potential, not just the changes in the IPSP's, as illustrated in Fig. 9, *A–C*. These equilibrium potentials are shown in Fig. 9, *A–C* but are more accurately determined by the plotted curves of Fig. 9*D*, each of which was defined in a few seconds. The points so obtained for the membrane potentials at which the curves of Fig. 9*B* cut the zero line for the IPSP—that is, the equilibrium potential—are plotted in Fig. 9*E* to show the slow time course of its recovery after a sodium injection. A particularly strong contrast between the effects of potassium and sodium injection is shown in Fig. 10, where there were alternate injections of sodium and potassium ions into the same motoneuron from a double-barreled electrode that was charged with potassium sulfate in one barrel and sodium sulfate in the other (*22*).

A crucial sequence of injections is illustrated in Fig. 11 (*23*). Two injections of sodium typically give the prolonged displacement of both the IPSP and its equilibrium potential in the direction of depolarization, as represented in Fig. 9*E* and Fig. 10, while after the chloride injection there is the large depolarizing displacement of both, and a quick recovery that is almost complete in 1 minute. When sodium plus chloride ions are injected by interbarrel current flow, there is a similar large displacement and fast recovery of both. The ionic composition of the cell after the sodium-plus-chloride injection differs in one important respect—the well-maintained level of intracellular potassium—from that after an injection of sodium alone. Evidently the large decrease in intracellular potassium that eventuates from the sodium injection is the crucial causative factor in the slowing of recovery of the inhibitory equilibrium potential from its depolarized displacement, which apparently is due in large part to a slowing in the decline of the raised level of intracellular chloride.

In order to account for the various effects of ion and salt injections on the IPSP, it has been postulated (*9*, *23*)

that at low levels of intracellular potassium there is activation of an inward pumping mechanism for potassium ions plus chloride ions in approximately equivalent amounts. At low levels of intracellular potassium this pump would maintain the intracellular chloride above the level at which there is diffusional equilibrium across the membrane. The continual influx of chloride against its electrochemical gradient thus accounts for the slow decline of the depolarizing displacement of the IPSP that always occurs (Figs. 9*E*, 10, and 11) when an increase in intracellular chloride is associated with a large decrease in intracellular potassium, and under no other circumstances. It has been possible to develop a mathematical formulation that gives a satisfactory quantitative explanation of this effect (*23*).

Since potassium ions are normally at such a high level in nerve cells, the ion injection procedures cannot produce large changes in their concentration, and hence have been indecisive in respect of evidence for or against potassium ion permeability as a contributory factor in production of the IPSP. Nevertheless, an assessment of a relatively large contribution from potassium ion permeability can be made on the basis of the following evidence (*9, 23*). The equilibrium potential for potassium is more hyperpolarized than the resting membrane potential by about 20 millivolts; the equilibrium potential for inhibition is similarly in the direction of hyperpolarization, but less so, probably by about 6 to 10 millivolts; the equilibrium potential for chloride is probably slightly in the direction of depolarization, on account of the operation of the postulated inward chloride pump. These considerations suggest that the permeability of the activated inhibitory membrane for potassium ions is at least half that for chloride ions; and the simplest assumption is equality, the permeability being determined solely by hydrated-ion size, but for cations as well as anions, which is of course sufficient to exclude the large hydrated sodium ions.

Models of Inhibitory Synapses

On this basis the action of inhibitory synapses on a motoneuron can be shown in the formal electrical diagram of Fig. 12*D*, where a ganged switch would throw into the circuit across the membrane both the chloride- and the potassium-controlled elements, with potentials of −70 and −90 millivolts, respectively (*24*). Together these elements would give an effective battery of −80 millivolts, which corresponds to the equilibrium potential for inhibition.

The equilibrium potential of −80 millivolts for the IPSP could only be attained if the pores in the inhibitory membrane were small enough to effect a virtually complete exclusion of sodium ions; otherwise the sodium ionic flux resulting from the synaptic action would produce depolarization and excitation. In fact the fundamental difference between excitatory and inhibitory synapses is that sodium permeability is high with the former and negligible with the latter (*9, 25*). A small permeability to bromate ions was reported, with inhibitory synapses, in the snail's brain (*26*); otherwise the anion permeability tests showed no intermediate behavior, there being a sharp differentation between the permeable and the impermeable (*18–21*); therefore it must be postulated that the pores or channels across the membrane have a uniform

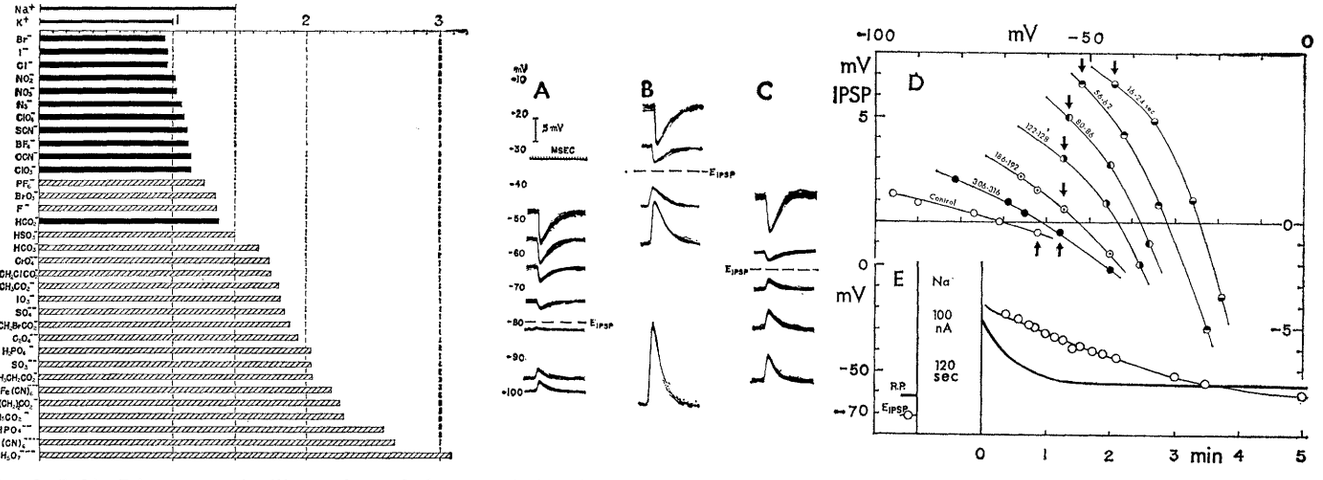

Fig. 8 (left). Diagrammatic illustration of the correlation between the size of ions in the aqueous solution and the effects of their injection upon the IPSP. The length of the bars indicates ion size in the aqueous solutions as calculated from the limiting conductance in water. (Solid bars) Anions effective in converting the IPSP into the depolarizing response, as in Fig. 7, *B*, *I*, and *J*; (hatched bars) anions not effective, as in Fig. 7*F*. Sizes of K^+ and Na^+ ions in the hydrated state are shown above the length scale; the size of the K^+ ion is taken as the unit for representing the size of other ions (Ito, Kostyuk, and Oshima, *19*). Fig. 9 (right). In *A*, the IPSP's of Fig. 5*G* are shown arranged according to their membrane potentials on the scale indicated by short horizontal lines at left; the equilibrium potential for the IPSP is shown by the dashed line. *B* shows the situation 5 to 40 seconds after the passage of a depolarizing current of 5×10^{-8} ampere for 90 seconds through the microelectrode (filled with 0.6*M* Na_2SO_4); the IPSP's are arranged on the same scale as in *A*, the E_{IPSP} being now −35 millivolts. *C* shows, on the same scale, the IPSP's obtained during partial recovery at 3 to 4 minutes after the electrophoretic injection, with the E_{IPSP} at −66 millivolts. *D* and *E* show the effect of intracellular injection of Na^+ on the IPSP. The injection of Na^+ ions was made from one barrel of a double electrode, filled with 1.2*M* Na_2SO_4, by a current of 10×10^{-8} ampere for 120 seconds. The points on each curve in *D* were determined by recording the IPSP's over a range of membrane potentials, as in *A–C*. The curve furthest to the left represents the initial control observations; the other curves were obtained at the intervals indicated (in seconds) after cessation of the Na^+ injection. The summits of the IPSP's were plotted as ordinates against the membrane potentials as abscissas, and the E_{IPSP}'s can be read off directly as the membrane potentials at which the curves cross the zero IPSP line. The arrows indicate the points obtained when the membrane potential was not displaced by the applied current pulses. In graph *E* the values for E_{IPSP} before and after the injection are plotted; the resting membrane potential is shown by the solid line (Eccles, Eccles, and Ito, *22*).

size. It is difficult to envisage that channels so accurately formed can be brought into existence for one thousandth of a second through the whole thickness of the membrane. A more attractive postulate is that the pores are built into the membrane structure and are plugged, as shown in Fig. 12*A*, the action of the inhibitory transmitter being momentarily to displace the plug, as in *B*. This device could also occur for the excitatory synapses, but, as demonstrated by the sizes of the penetrating cations, the pores have about twice the diameter of the pores in Fig. 12 (*9*). One further important variant on the ionic permeability of pores is the possible existence of fixed charges

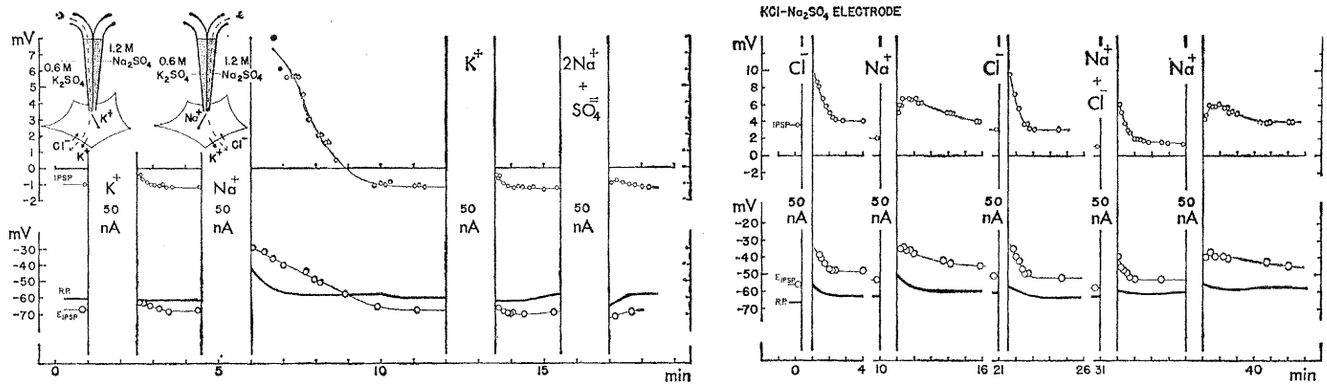

Fig. 10 (left). Effect of intracellular injections of Na^+ and K^+ on the IPSP responses of a motoneuron. The ion injections were made from a double microelectrode (inset diagrams) by means of a 90-second current flow, as indicated by the widths of the columns. All the observations are plotted on the time scale shown at bottom. The upper series of graphs show the potentials (top scale at left) for the summits of IPSP's. The IPSP was of the usual hyperpolarizing type (shown by negative sign of the voltage scale) at the start of the series and after recovery from each injection. The two curves in each of the lower graphs are plotted on the voltage scale shown at bottom left, and give the intracellular potential. The heavy curve represents the membrane or resting potential; each of the plotted points on the other curve gives a measurement for E_{IPSP}, the equilibrium potential for the IPSP. With the fourth injection the current flowed from the Na_2SO_4-filled barrel to the K_2SO_4-filled barrel, thus injecting ($2Na^+ + SO_4^{--}$). The two solid circles in the graph at left for the IPSP series (top row) just after the injection of Na^+ indicate that spike potentials were generated by the large depolarizing IPSP's; the plotted values were estimated from the steepness of the rising slopes of these IPSP's. After the injection of Na^+ or ($2Na^+ + SO_4^{--}$), recording was through the K_2SO_4-filled barrel; after the injection of K^+, recording was through the Na_2SO_4-filled barrel (Eccles, Eccles, and Ito, *22*). Fig. 11 (right). Effects of various ion and salt injections on the IPSP. One barrel of the double microelectrode was filled with 3*M* KCl, the other, with 1.2*M* Na_2SO_4. After the injection of Na^+ ions the recording was made through the barrel filled with KCl, and after the injection of Cl^- and $Na^+ + Cl^-$ through the barrel filled with Na_2SO_4. The effects of the various ion and salt injections are plotted as described for Fig. 10, but there are several gaps in the time scale, as indicated (for further description, see text) (Eccles, Eccles, and Ito, *23*).

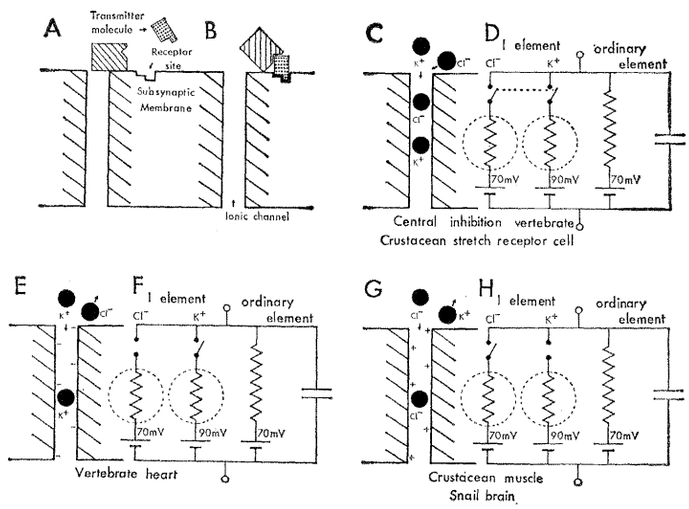

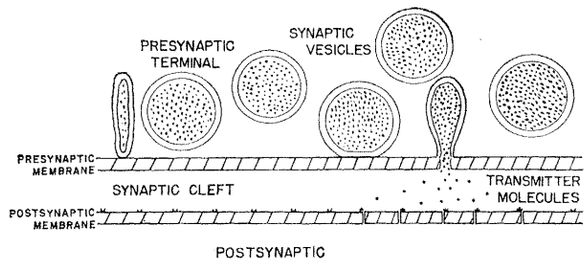

Fig. 12 (left). Diagrams summarizing the hypotheses relating to the ionic mechanisms employed by a variety of inhibitory synapses in producing IPSP's. *A*, *B*, Schematic representation of the way in which a synaptic transmitter molecule could effect a momentary opening of a pore in the subsynaptic membrane by causing the lifting of a plug. In *B* the transmitter molecule is shown in close steric relationship both to a receptor site and to the plug, which has been pulled away from the orifice of the pore. As a consequence, ions can move freely through pores in the subsynaptic membrane for the duration of the transmitter molecule's action upon it (Eccles, *35*). *C* is a schematic representation of a pore through an activated inhibitory subsynaptic membrane, showing the passage of both chloride and potassium ions that is postulated for IPSP production at central inhibitory synapes. *D* is a diagram resembling Fig. 5*F*, but showing the inhibitory element as being composed of potasium and chloride ion conductances in parallel, each with batteries given by their equilibrium potentials (Fig. 3*A*), and as being operated by a ganged switch, closure of which symbolizes activation of the inhibitory subsynaptic membrane. *E*, *F* and *G*, *H* represent the conditions occurring at inhibitory synapses where there is predominantly potassium ion conductance, as with the vertebrate heart, or predominantly chloride ion conductance, as with crustacean muscle or cells in the brain of a snail. It is assumed that the pores are restricted to cation or anion permeability by the fixed changes on their walls, as shown (Eccles, *24*, *32*). Fig. 13 (right). Diagrammatic representation of a portion of a synaptic cleft, with synaptic vesicles in close proximity in the presynaptic terminal and one discharging the transmitter molecules into the synaptic cleft. Some of these molecules are shown combined with receptor sites on the subsynaptic membrane, with consequent opening up of pores through that membrane.

on the walls of the pore that has been suggested by Fatt (*27*). As shown in Fig. 12, *E* and *F*, fixed negative charges would repel negatively charged particles and so would cause the pores to become impermeable to anions, and, conversely, fixed positive charges would give cation impermeability (Fig. 12, *G* and *H*). This selective effect of charged pores would provide the simplest explanation of the finding that some inhibitory actions are almost exclusively due to cation permeability [for example, the vagal inhibition on the heart is due to potassium permeability (Fig. 12, *E* and *F* (*28*)] and others, largely anionic, are due to chloride [for example, inhibition on crustacean muscle (*27*) and on nerve cells in the snail's brain (Fig. 12, *G* and *H*) (26)].

Conclusions

In conclusion, Fig. 13 summarizes diagrammatically the detailed events which are presumed to occur when an impulse reaches a presynaptic terminal, and which we would expect to see if electron microscopy can be developed to have sufficient resolving power. Some of the synaptic vesicles are in close contact with the membrane, and one or more are caused by the impulse to eject their contained transmitter substance into the synaptic cleft. Diffusion across and along the cleft, as shown, would occur in a few microseconds for distances of a few hundred angstroms. Some of the transmitter becomes momentarily attached to the specific receptor sites on the postsynaptic membrane, with the consequence that there is an opening up of fine channels across this membrane—that is, the subsynaptic membrane momentarily assumes a sieve-like character. The ions, chloride and potassium, move across the membrane thousands of times more readily than normally, and this intense ionic flux gives the current that produces the IPSP and that counteracts the depolarizing action of excitatory synapses, so effecting inhibition.

References

1. L. G. Brock, J. S. Coombs, J. C. Eccles, "Action potentials of motoneurones with intracellular electrode," *Proc. Univ. Otago Med. School* **29**, 14 (1951).
2. ———, "The recording of potentials from motoneurones with an intracellular electrode," *J. Physiol. London* **117**, 431 (1952).
3. J. S. Coombs, D. R. Curtis, J. C. Eccles, "The interpretation of spike potentials of motoneurones," *ibid.* **139**, 198 (1957).
4. ———, "The electrical constants of the motoneurone membrane," *ibid.* **145**, 505 (1959); J. S. Coombs, J. C. Eccles, P. Fatt, "The electrcial properties of the motoneurone membrane," *ibid.* **130**, 291 (1955).
5. J. C. Eccles, *The Physiology of Nerve Cells* (Johns Hopkins Press, Baltimore, 1957).
6. A. L. Hodgkin, "The ionic basis of electrical activity in nerve and muscle," *Biol. Rev. Cambridge Phil. Soc.* **26**, 339 (1961); ———, "Ionic movements and electrical activity in giant nerve fibres," *Proc. Roy. Soc. London* **B148**, 1 (1958); ——— and A. F. Huxley, "A quantitative description of membrane current and its application to conduction and excitation in nerve," *J. Physiol. London* **117**, 500 (1952); A. L. Hodgkin and B. Katz, "The effect of sodium ions on the electrical activity of the giant axon of the squid," *ibid.* **108**, 37 (1949); A. F. Huxley, "Electrical processes in nerve conduction," in *Ion Transport across Membranes*, H. T. Clarke, Ed. (Academic Press, New York, 1954), pp. 23–34; ———, "Ion movements during nerve activity," *Ann. N.Y. Acad. Sci.* **81**, 221 (1959).
7. J. S. Coombs, D. R. Curtis, J. C. Eccles, "The generation of impulses in motoneurones," *J. Physiol. London* **139**, 232 (1957).
8. J. C. Eccles, *The Neurophysiological Basis of Mind: The Principles of Neurophysiology* (Oxford Univ. Press, London, 1953).
9. ———, *The Physiology of Synapses* (Springer, Berlin, 1964).
10. T. Araki and C. A. Terzuolo, "Membrane currents in spinal motoneurones associated with the action potential and synaptic activity," *J. Neurophysiol.* **25**, 772 (1962).
11. J. S. Coombs, J. C. Eccles, P. Fatt, "Excitatory synaptic action in motoneurones," *J. Physiol. London* **130**, 374 (1955).
12. D. R. Curtis and J. C. Eccles, "The time courses of excitatory and inhibitory synaptic actions," *ibid.* **145**, 529 (1959).
13. J. S. Coombs, J. C. Eccles, P. Fatt, "The inhibitory suppression of reflex discharges from motoneurones," *ibid.* **130**, 396 (1955).
14. J. C. Eccles, "The behaviour of nerve cells," in *Ciba Symposium on the Neurological Basis of Behaviour*, G. E. W. Wolstenholme and C. M. O. O'Connor, Eds. (Churchill, London, 1958), pp. 28–47.
15. J. S. Coombs, J. C. Eccles, P. Fatt, "The specific ionic conductances and the ionic movements across the motoneuronal membrane that produce the inhibitory postsynaptic potential," *J. Physiol. London* **130**, 326 (1955).
16. J. C. Eccles, "The nature of central inhibition," *Proc. Roy. Soc. London* **B153**, 445 (1961).
17. J. S. Coombs, J. C. Eccles, P. Fatt, "The action of the inhibitory synaptic transmitter," *Australian J. Sci.* **16**, 1 (1953).
18. T. Araki, M. Ito, O. Oscarsson, "Anion permeability of the synaptic and non-synaptic motoneurone membrane," *J. Physiol. London* **159**, 410 (1961).
19. M. Ito, P. G. Kostyuk, T. Oshima, "Further study on anion permeability in cat spinal motoneurones," *ibid.* **164**, 150 (1962).
20. Y. Asada, "Effects of intracellularly injected anions on the Mauthner cells of gold fish," *Japan J. Physiol.* **13**, 583 (1963).
21. T. Araki, personal communication (1963).
22. J. C. Eccles, R. M. Eccles, M. Ito, "Effects of intracellular potassium and sodium injections on the inhibitory postsynaptic potential." *Proc. Roy. Soc. London*, in press.
23. ———, "Effects produced on inhibitory postsynaptic potentials by the coupled injections of cations and anions into motoneurones, *ibid.*, in press.
24. J. C. Eccles, "Excitatory and inhibitory synaptic action," *Ann. N.Y. Acad Sci.* **81**, 247 (1959).
25. A. Takeuchi and N. Takeuchi, "On the permeability of the end-plate membrane during the action of transmitter," *J. Physiol. London* **154**, 52 (1960).
26. G. A. Kerkut and R. C. Thomas, "The effect of anion injection and changes in the external potassium and chloride concentration on the reversal potentials of the IPSP and acetylcholine," *Comp. Biochem. Physiol.*, in press.
27. J. Boistel and P. Fatt, "Membrane permeability change during inhibitory transmitter action in crustacean muscle," *J. Physiol. London* **144**, 176 (1958).
28. W. Trautwein and J. Dudel, "Zum Mechanismu der Membranwirkung des Acetylcholin an der Herzmuskelfaser," *Arch. Ges. Physiol.* **266**, 324 (1959).
29. R. Jung, "Allgemeine neurophysiologie," in *Handbuch der Inneren Medizin* (Springer, Berlin, 1953), pp. 1–181.
30. S. L. Palay, "The morphology of synapses in the central nervous system," *Exptl. Cell Res. Suppl.* **5**, 275 (1958).
31. L. H. Hamlyn, "An electron microscope study of pyramidal neurons in the Ammon's horn of the rabbit," *J. Anat. London* **97**, 189 (1963).
32. J. C. Eccles, "The synaptic mechanism of post-synaptic inhibition," in *Nervous Inhibition*, E. Florey, Ed. (Pergamon, New York, 1961), pp. 71–86.